Eduardo Aguirre de la Torre
Miguel de Cervantes 120, Complejo industrial Chihuahua. C.P. 31109
Tel: 439-11-00
E-mail: eduardo.aguirre@cimav.edu.mx

Umberto Afeltra
Via Roma 200-25020 Dello (Brescia) Italia
Tel: 439-11-00
E-mail: uafeltra@hayez-lemmerz.com

Cynthia Gómez Esparza
Miguel de Cervantes 120, Complejo industrial Chihuahua. C.P. 31109
Tel: 439-11-00
E-mail: cynthia.gomez@cimav.edu.mx

Javier Camarillo Cisneros
Miguel de Cervantes 120, Complejo industrial Chihuahua. C.P. 31109
Tel: 439-11-00
E-mail: javier.camarillo@cimav.edu.mx

Raúl Pérez Bustamante
Miguel de Cervantes 120, Complejo industrial Chihuahua. C.P. 31109
Tel: 439-11-00
E-mail: raul.perez@cimav.edu.mx

Roberto Martínez Sánchez
Miguel de Cervantes 120, Complejo industrial Chihuahua. C.P. 31109
Tel: 439-11-00
E-mail: roberto.martinez@cimav.edu.mx

EFFECT OF AL-5TI-B ON THE MICROSTRUCTURE AND MECHANICAL PROPERTIES OF THE A356 ALUMINUM ALLOY

Abstract

A356 aluminum alloy automotive wheels, 17-inch in diameter, were produced by low-pressure die casting (LPDC). Contents of Al-5Ti-B (ATB) master alloy were added from 0 to 0.79 wt.%. Microstructural and mechanical properties were evaluated under industrial casting process conditions. The obtained results from mechanical testing provide evidence that additions of 0.13 and 0.27 wt.% of ATB have an improvement on the mechanical performance of the automotive wheels. This can be compared with the use of grain refiner's higher concentrations leading to a significant reduction in the cost-benefit ratio for the manufacturing of A356 automotive wheels.

Keywords: Al-5Ti-B; Grain refiner; Industrial process; Automotive; Wheels; A356

Introduction

Aluminum alloys are widely used in the automotive, aeronautic and aerospace industries due to their high strength-to-weight ratio compared to that of steels and to their capability of being heat treated to improve their mechanical properties. These characteristics make them excellent materials to be used in structural applications as outlined (Ref 1). Regarding the automotive industry, the use of Al-Si alloys has allowed the production of lightweight wheels with complex geometries. The low-pressure die casting (LPDC) process is considered to be of special interest because it offers the advantage of obtaining higher quality products due to the reduction of porosity and allows a larger-scale production than in the case of gravity die casting (GDC) processes (Ref 2). Additionally, the mechanical performance of the aluminum alloys produced with casting can be enhanced by using grain refiners, which promote the formation of finer grains and improve the mechanical behavior of the final products.

The grain refiner effect based on Ti, B and the compounds they form has previously been studied by several research groups from a variety of techniques mainly based in GDC as well as LPDC. Industrially, grain refiners are commonly used in the form of bars directly added to the molten metal, which is an economic method compared to that with salt addition. The efficiency of the refiner ATB on grain size reduction can be optimized by an adequate selection of the contact time with the molten metal. Intervals of the refiner effectiveness from 30 to 60 min have been reported, pure aluminum (Ref 3), as in the case of Al-Si hypoeutectic alloys (Ref 4). The fading mechanism of grain refinement using ATB in Al-Si indicated its effectiveness before 60 minutes of contact time. In all cases, the optimum time for grain refinement of Al-Si alloys is influenced by the presence of borides along grain boundaries.

Therefore, the use of grain refiners as well as their effect on the mechanical properties of industrial finished products has been scarcely investigated. The A356 alloy, commonly used in the automotive industry (Ref 5), has been selected to study the effects of ATB grain refiner concentration on its microstructure and mechanical properties.

The amounts of the grain refiner used in this research are in the range of those traditionally used in the industrial process (0.2 - 0.5 wt. %). However, they significantly differ from the concentrations used in this kind of investigations at a laboratory scale where the grain refiner amounts, which are higher than 1 %, are employed (Ref 6, 7).

The effectiveness of the ATB grain refining in the A356 automotive wheels production of an industrial route is studied in this research in order to optimize the processing conditions for the optimal mechanical performance in final products and the subsequent effect in the production costs of A356 automotive wheels.

EXPERIMENTAL PROCEDURE

Production of A356 alloy.

15-kg ingots of commercial A356 alloy, whose chemical composition is shown on Table I, were used for the automotive wheel production in LPDC. Alloy loads were melted in a high-efficiency gas melting furnace at 760°C. The molten A356 alloy (450 kg) was poured into a container of transference and then it was subsequently degassed. The degassing process was performed with N2 using a flow of 24 lt/ min for 5 min. Thus, the ATB was added to the degassed melting using bars of 200 g. Molten metal was stirred for a period of 0.5 min and transferred, at 710°C, to the holding furnace of a LPDC machine. Injection molding material was taken from the bottom of the holding furnace at a pressure of 0.04 MPa and solidification was conducted at 0.1 MPa. Fifteen wheels, per each composition (see Table II), were fabricated in a 5-spoke wheel-like permanent mold (which was made of steel and coated with a ceramic coating) across a time interval of 4 min per task.

Table I. Chemical composition of A356 alloy.

Alloying element	Si	Fe	Mg	Ti	Sr	Cu	Mn	Zn	Ni	Cr	Al
Wt. %	6.398	0.098	0.249	0.097	0.010	0.001	0.003	0.006	0.012	0.001	Bal
±	0.421	0.005	0.015	0.011	0.001	0.000	0.000	0.002	0.001	0.001	

Wheels that correspond to M0, M20, M40 y M60 from each group were selected after every 20 min in order to analyze the effect of the interaction time between the grain refiner (ATB) and the A356 alloy. Compositions and nomenclatures are summarized on Table II. Automotive wheels in the as-casting condition were heat treated with solubilization at 540°C during 3 h. They were not only quenched in water at 60°C but also artificially aged at 165°C for 3 h (T6 condition).

Table II. Nomenclature of groups and individual samples.

Groups	Number of bars added (200 g ATB)	Content of ATB (wt. %)	Wheel identification			
			M0	**M20**	**M40**	**M60**
G0	0	0.00	G0-M0	G0-M20	G0-M40	G0-M60
G3	3	0.13	G3-M0	G3-M20	G3-M40	G3-M60
G6	6	0.27	G6-M0	G6-M20	G6-M40	G6-M60
G9	9	0.40	G9-M0	G9-M20	G9-M40	G9-M60
G12	12	0.53	G12-M0	G12-M20	G12-M40	G12-M60
G15	15	0.66	G15-M0	G15-M20	G15-M40	G15-M60
G18	18	0.79	G18-M0	G18-M20	G18-M40	G18-M60

`

Microstructural characterization and mechanical properties

Chemical, mechanical and microstructural analyses were performed in each of the five spokes of the automotive wheels fabricated. Fig. 1 illustrates the section of wheels used for these analyses. Chemical composition of the produced pieces was determined in a FSQ Spectrometer. Microstructural characterization, where optical and scanning electron microscopy was carried out using an OLYMPUS/GX-54 optical microscope and a JEOL/JSM-5800-LV scanning electron microscope equipped with energy-dispersive X-ray spectrometer (EDS). Secondary dendrite arm spacing (SDAS) analyses are reported as the average value obtained from 40-50 measurements in each case. Grain size analysis was carried out with the standard linear intercept method. Mechanical properties were evaluated with tensile tests based on ASTM E8 (Fig. 1b). Experiments were performed in an INSTRON/337 universal testing machine at room temperature using a constant crosshead speed of 0.01 mm/s. Charpy impact tests were carried out in a TINIUS OLSEN/ IMPACT 104 machine based on ASTM E23 (Fig. 1c). Hardness was measured under 200 g load with 14.2 s dwell time on a WILSON/K10 Brinell hardness tester.

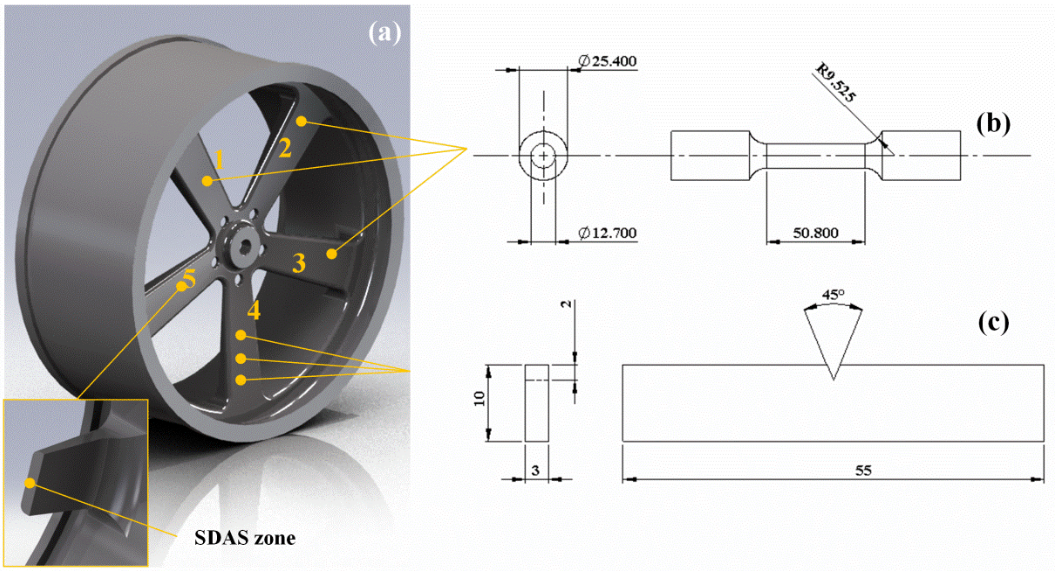

Figure 1. (a) Schematic representation of zones selected in A356 automotive wheels to perform chemical analyses, microstructural characterization and mechanical evaluation. (b) Dimensions of the samples for tensile test. (c) Dimensions of the samples for impact test. Dimensions are given in mm.

Results and discussion

The results of chemical analyses carried out in samples are presented in Fig. 2. Boron is estimated in a Ti/B ratio of 5:1. The amount of Ti is less than 0.1 wt. % in the reference alloy (G0) while it is in the interval of 0.11 to 0.15 wt.% in groups with the master alloy. Concentration of Ti increases as a function of the amount of ATB based on proportions as it is shown on Table II. It is very remarkable that the efficiency of the grain refiner is influenced by the amount of Ti in the as-received A356 alloy. The grain size reduction begins in alloys because the Ti content is from 0.005 to 0.078 wt. %. (Ref 3, 8).

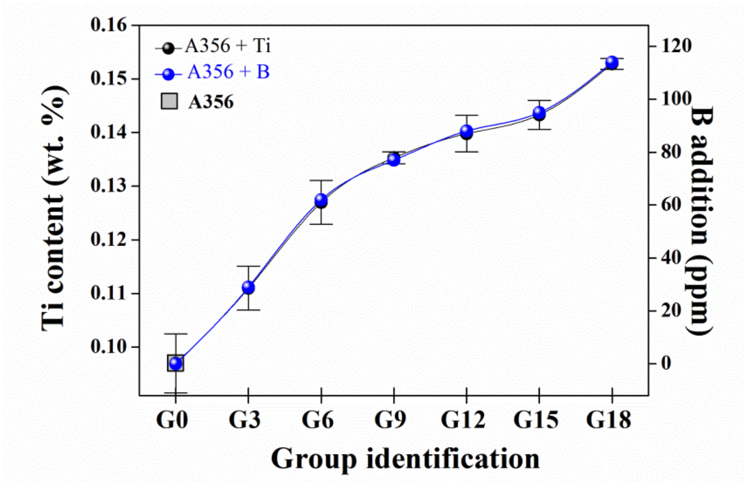

*Figure. 2. Concentrations of Ti for each group as a function of ABT content based on values presented in Table I. *G-0 indicates the alloy of reference.*

Fig. 3 presents the microstructure of the G18 group in the as-cast (Figs. 3a,b) and T6 condition (Figs. 3c,d). Microstructures show a difference in the size and shape of silicon particles as a result of the T6 heat treatment. It is observed α (Al) primary phase with dendrite morphology; whilst the Al-Si eutectic, which was changed in fine spheroidized Si particles homogeneously dispersed in the aluminum matrix, appears in grey tone.

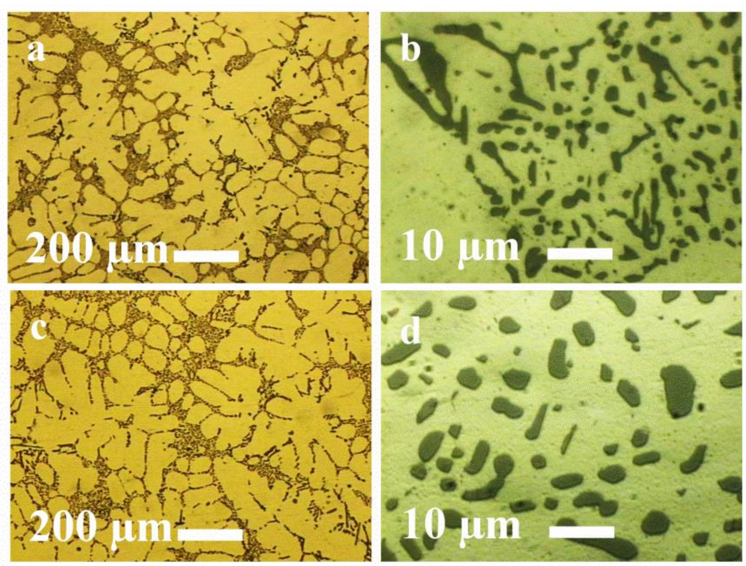

Figure 3. Microstructures of G18 group (a,b) As-cast and (b-c) T6 condition. (b) Magnified view of (a). (d) Magnifiew view of (c).

Fig. 4 shows backscattering electron micrograph obtained by SEM corresponding to the sample G18-M60 in the T6 condition. An EDS elemental map of three alloying elements

(Al, Fe and Si) is presented. The Al-matrix (colored in green), the presence of irregular-shaped phases of Si (colored in blue) as well as needle-shaped iron rich phases (colored in blue) are observed. The absence of Ti in this analysis is attributed to the very low Ti concentration and the limitations attributed for SEM analysis in the elemental characterization.

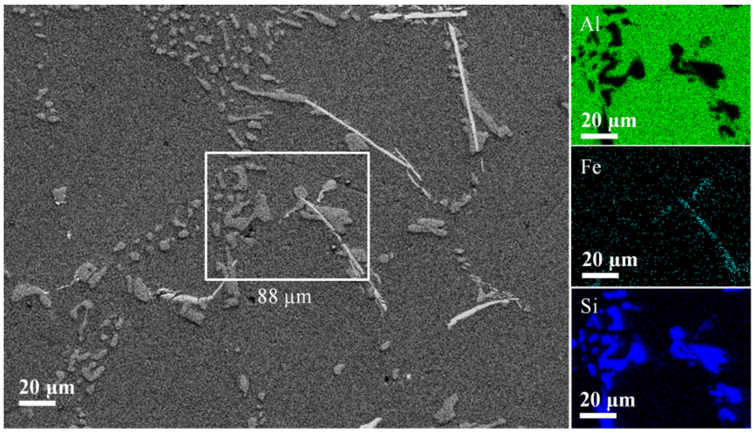

Figure 4. SEM micrograph of the sample identified as G18-M60 (left) and EDS elemental maps (right) which evidence the presence of Al, Fe and Si. Elemental mapping area, 88 mm x 75mm, is indicated by the white rectangle in the microstructure.

Observations corresponding to samples M60 were carried out by optical analysis. Fig. 5 presents the secondary SDAS measurements of samples in the T6 condition. There is a significant drop of SDAS in samples G3-M60 and G6-M60. An apparent null effect of the refiner is observed in samples from G9-M60 to G18-M60. It is noteworthy that observations with optical microscopy as well as SDAS and grain size measurements (inset shown in Fig.5) were made after 60 min of contact time between the refiner and the molten alloy (sample M60, Table II). A rapid SDAS reduction in the sample G6-M60 in the T6 condition and an apparent null effect of the refiner in samples from G9-M60 to G18-M60 is observed. Regarding the grain size for the same condition, a slight reduction was noticed as a function of the amount of ATB. As it can be observed, a grain size reduction of about 14% is achieved in group G18 in consideration to the reference alloy (G-0). According to the observations carried out by Yu *et al.* (Ref 6), there is a close relationship between SDAS and grain size due to the area variation of grain boundaries. However, such relationship was not observed in this investigation.

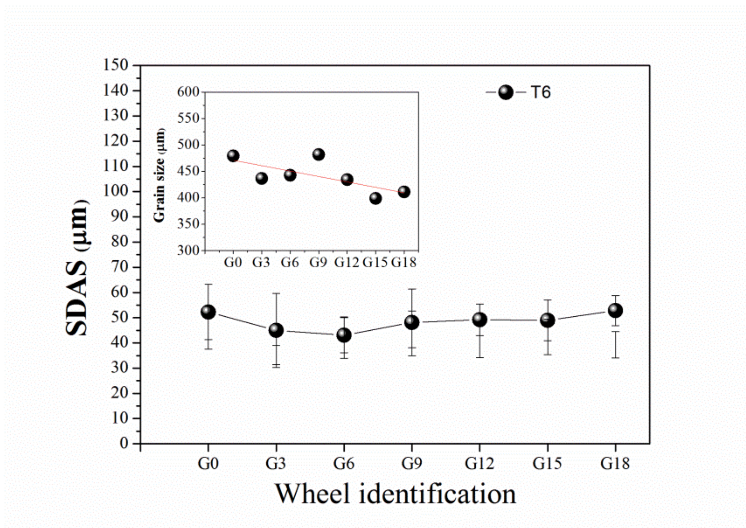

Figure 5. Variation of SDAS as a function of the refiner amount in the heat-treated samples, T6. The inset shows the results of grain size measured in the samples under T6 heat treatment.

As it can be observed, changes in SDAS caused by the refiner are different from those observed in the grain size. Measurements show the SDAS 52.22 µm value for the G0 group whilst the G18 displays the SDAS 52.87 value. Therefore, it indicates no effect in the SDAS with the maximal ATB addition used in this research. However, a visible effect in the efficiency of the ATB grain refiner can be observed in the G3 and G6 groups where a lower value for SDAS was presented by the G3 group with a dendritic spacing of 44.98 µm.

Variations in SDAS and grain size cannot be attributed to a decrease on the grain refiner efficiency as a consequence of the poisoning effect of elements such as Zr and Cr as it has previously been reported by Jones *et al.* (Ref 3). This observation is supported by the contents of these alloying elements which do not justify this theory. Besides, the content of Ti found in the samples does not present a variation that justifies the presence of fading. This can be related to that in the industrial production method since the settling rate of phases containing Ti is similar to the production rate avoiding, in this way, high concentrations of these alloying elements at bottom of the holding furnace as time passes.

Fig. 6 shows results from the Charpy impact test as the function of ATB for those samples in the T6 condition. In comparison with the reference group (GO), only the G3 and G6 groups exhibit an increase in the impact energy. The rest of the samples show a decrease in the energy impact with increases in the ATB concentration. An inverse correlation between SDAS, the grain size and the absorbed energy has been reported. It is attributed to a finer microstructure obtained by increasing the ATB content (Ref 9).

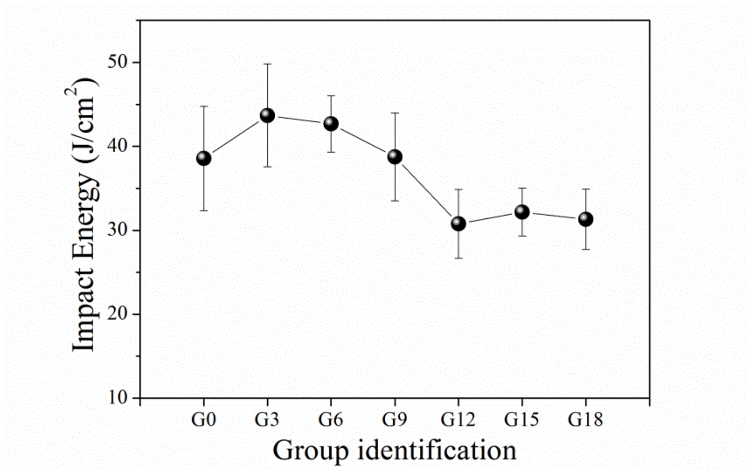

Figure 6. Results of mechanical testing under Impact of the A356 as function of grain refiner content.

Results from hardness (HB) measurements are displayed in Fig. 7. Results come from samples in the as-cast and T6 condition where a noticeable increase in hardness values for all groups is shown due to the effect of heat treatment. In both cases, the hardness of group G3 slightly decreases, about 1 unit, compared with the group G0. HB was reduced from 86.75 to 85.76. However, as the ATB concentration increases, the curve presents a slightly ascendant behavior in both conditions. The highest value of hardness (88.65 HB) for the T6 heat treated samples was observed in the group G18. Therefore, hardness is not practically altered by ATB in the range of concentrations used in this investigation. The achieved hardness in samples is due to the conditions used in heat treatment rather than the effect caused by the ATB concentration in the A356 aluminum alloy.

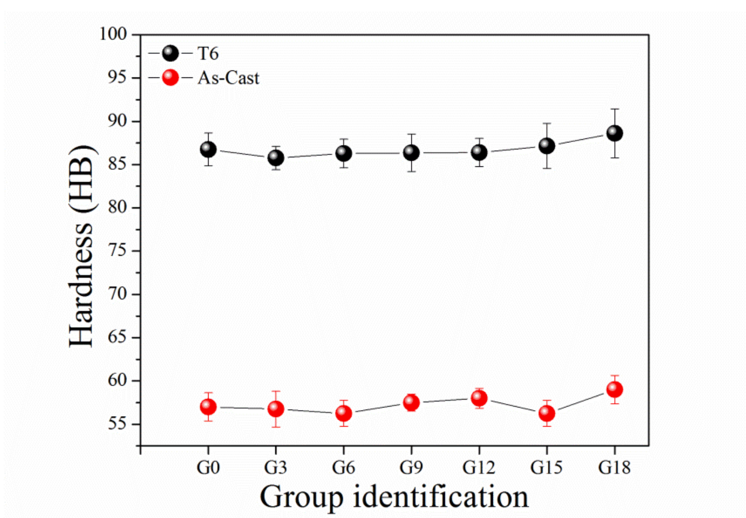

Figure 7. Hardness results in the as-cast and T6 condition. Results are presented as function of the ATB concentration in the A356 aluminum alloy.

Representative stress-strain curves, as function of the ATB content are given in Fig. 8. A deeper analysis about the ductility and strength of the samples is shown in Fig. 9. Fig. 9a shows the results of the function of the grain refiner content and the function of the retention time (Fig. 9b). According to the results of the grain refiner concentration function, there is a drop of the yield strength (σy) as the amount of ATB increases up to group G6. A slight increase in σy is observed as the refiner content is increased in this group. However, the only group that exhibits higher σ_y than that of the reference is G18. The enhancement of the mechanical behavior, due to grain size reduction, is reflected in the improvement of σ_y only for groups G12 and G18. In the same way, the maximum strength (σ_{max}) presents a clear tendency of decreasing as the ATB content increases but a slight increase of elongation to fracture (ε) in group G3 is observed. Nevertheless, where higher amounts of ATB are present, a significant reduction of this parameter is observed. Ductility considerably decreases from group G6. The same behavior was observed by Zhu et al. (Ref 7) where it is studied the effect of additions of Al-Ti-B master alloy on mechanical properties of A356 alloys and found that the mechanical properties of refined samples improve steadily and then slightly decrease under both as-cast and T6 heat-treated conditions. However, the variations in mechanical properties are not significantly important. The tensile tests show that the elongation of the composites after T6 treatment decreases within a narrow range, which is related to the precipitates presence after ageing treatment. As the precipitates are growing up and added, the movement of dislocations needs to cross the precipitation not only because it increases the resisting force of dislocation movement but also because it increases the difficulty of grain boundary sliding. Thus, the strength of the composites is enhanced, while the elongation is reduced (Ref 10).

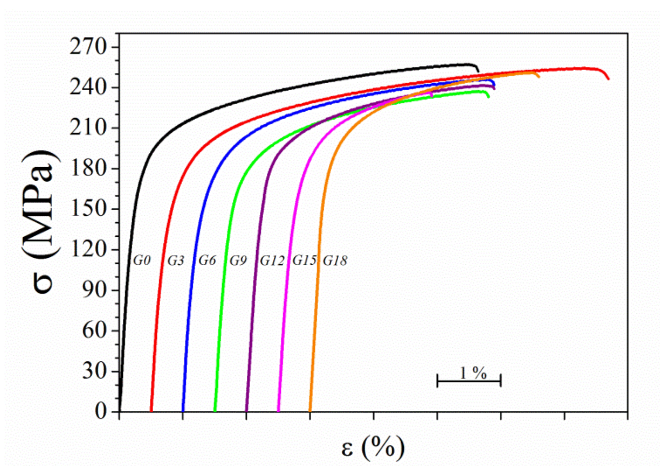

Figure 8. Stress-strain curves of the A356 alloy as function of the ATB content.

The analysis of the effect of retention time (in the chamber of LPDC system), on the tensile behavior of the wheels, is shown in Fig. 9. In a similar way, σ_y shows very small differences. This difference is just about 5% when the lowest and highest values are taken into account. Additionally, all values lie within the standard deviations found for the set of the evaluated pieces. Therefore, σ_y remains constant when varying the time during which the alloy is kept in the retention furnace. On the other hand, a small variation of about 2% among the tensile strength of samples M0, M20 and M40 is also observed. σmax in M40 and M60 groups present a variation around 3%. Regarding elongation to fracture, not only a slight decrease of about 12.7% in M20 is observed compared to M0 but also an increase of 14% between samples M40 and M60. However, a positive slop is seen from M20 to M60 and the differences between the lowest and highest values are very small. As a result, it can be considered that σy and σmax are constant, while ε varies negligibly as a function of the retention time. The three characteristics possess stability independently of the time due to the studied industrial process.

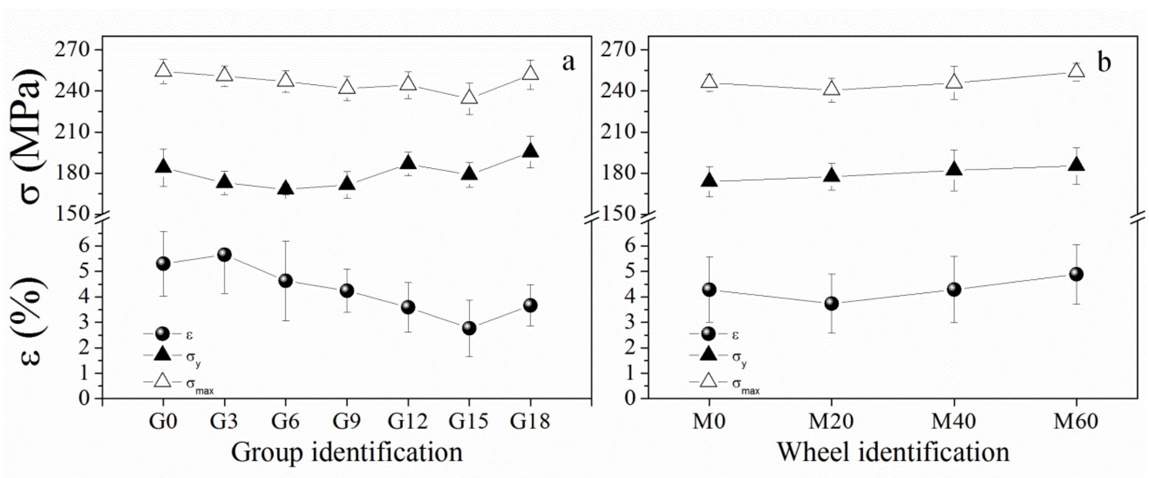

Figure 9. Mechanical behavior of A356 alloy as a function of the ATB content. (a) Analysis by group and (b) analysis by wheel.

The effect of ATB on the mechanical properties for the studied groups is not significant after being heat-treated. Therefore, the hardening effect reached due to grain size refinement, for the contents of the grain refiner used in this assignment, is negligible compared to that attained after the T6 condition. (Ref 7), reported the grain refinement effect on a A356 alloy in the as-cast and T6 condition, having found an increase in σ_y (108.3 MPa) and σ_{max} (189.3 MPa) after an addition of 2.5 wt. % of ATB, however, these values are below of those found for the A356 in the T6 condition (G0) used in this research, where σ_y and σ_{max} are 140.0 and 231.3 MPa respectively. From these observations and from Figs. 6 ,8 and 9, the fact that the effect of the ATB grain refiner in the mechanical performance of the A356 alloy is irrelevant after the T6 condition can be mentioned, at least in the experimental conditions (thermal cycle and amount of refiner added) used in this work. However, the use of grain refiners cannot be discarded because its presence favors the formation of equiaxed grains, reducing the porosity in the alloy as well as the ingot cracking (Ref 11).

It has been reported that prolonged retention times favor the presence of the fading phenomenon, which negatively affects the mechanical properties of the Al-Si alloys. This phenomenon is observed in systems of GDC in which molds filling are conducted for the upper part of the furnace (Ref 4). Additionally, particles concentration of (Al, Ti)B2 decrease 40 to 80 times from fist to last sample (Ref 12). This negatively affects the mechanical properties of samples due to the less amount of Ti available to react with B and form TiB2. However, due to filling of the automotive wheel molds in the LPDC retention furnaces is conducted from the bottom, this effect is minimized. Additionally, other phenomenon that negatively affects the mechanical properties of Al-Si alloys, which is influenced by the retention time, is the so-called poisoning effect (Ref 3). However, despite of the retention times used in this study, the contents of Cr in the A356 alloy do not justify this phenomenon. Therefore, the values of σ_y, σ_{max} and ε, which exhibit a positive slope, are influenced by the amount of ATB. Although the observed slop is positive, the variation among the values is very low. Considering the error bars, it is clear that the obtained values from the tension tests remain constant while varying the holding time.

From the previous results, observations indicate an efficient grain refinement in the A356 with Ti contents from 0.097 (Ti content in the as-received A356 aluminum alloy) to 0.13 wt. % (G3 group) for the manufacture of automotive wheels, leading to a subsequent significant reduction in the production costs of A356 aluminum alloy wheels.

Conclusions

- The effect of grain refiner (ATB) was investigated for concentrations in the interval of 0 – 0.79 wt. % after solution heat treatment at 540°C during 3 h, and artificially aged at 165°C for 3 h (T6 condition).
- Additions of the refiner up to 0.13 wt. % causes a decrease of SDAS in the A356 produced by LPDC, resulting in automotive wheels with higher elongation to fracture and higher absorbed impact energy.
- Mechanical properties of the A356 alloy modified with additions of ATB and studied after T6 condition, such as hardness, yield strength and tensile strength are not significantly altered with the ATB variations employed in this research.
- The fading effect in the studied alloys is significantly minimized due to manufacture of automotive wheels by LPDC where mold filling is performed from the bottom of the retention furnace.
- The reduction in the amount of the ATB represents a significant saving without notable changes in the mechanical properties of the A356 alloy here studied, whose chemical composition is the one shown in this research.

- The strengthening by grain refinement found in this alloy under the specific experimental conditions is minimum, and it has no comparison with the strengthening reached precipitation after T6 temper.

Acknowledgements

This research was supported by CONACYT (106658). Thanks to Redes Temáticas de Nanotecnología y Nanociencias, Reg. 0124623. Thanks to Red de Ciencia y Tecnología Espaciales Regs.0170962 and 0170617. Thanks to J. A. Hernandez-Gutierrez and K. Campos-Venegas for their valuable technical assistance.

References

[1] 1. G.S. Cole and A.M. Sherman, Light weight materials for automotive applications, *Materials Characterization*, 35(1), 1995, 3-9
[2] 2. F. Bonollo, J. Urban, B. Bonatto and M. Botter, Gravity and Low pressure die casting of aluminium alloys: A technical and economical benchmark, *Metallurgia Italiana*, 97(6), 2005, 23-32
[3] 3. G. Jones and J. Pearson, Factors affecting the grain-refinement of aluminum using titanium and boron additives, *Metallurgical and Materials Transactions B*, 7(2), 1976, 223-234
[4] 4. C. Limmaneevichitr and W. Eidhed, Fading mechanism of grain refinement of aluminum-silicon alloy with Al-Ti-B grain refiners, *Materials Science and Engineering: A*, 349(1-2), 2003, 197-206
[5] 5. G. Wang, L. Yan, G. Ren and Z. Zhao, Analyzing As-Cast Age Hardening of 356 Cast Alloy, *Journal of Materials Engineering and Performance*, 20(3), 2011, 399-404
[6] 6. L. Yu, X. Liu, Z. Wang and X. Bian, Grain refinement of A356 alloy by AlTiC/AlTiB master alloys, *Journal of Materials Science*, 40(14), 2005, 3865-3867
[7] 7. M. Zhu, G. Yang, L. Yao, S. Cheng and Y. Zhou, Influence of Al-Ti-B addition on the microstructure and mechanical properties of A356 alloys, *Rare Metals*, 28(2), 2009, 181-186
[8] 8. B.T. Sofyan, D.J. Kharistal, L. Trijati, K. Purba and R.E. Susanto, Grain refinement of AA333 aluminium cast alloy by Al-Ti granulated flux, *Materials and Design*, 31, Supplement 1(0), 2010, S36-S43
[9] 9. M. Merlin, G. Timelli, F. Bonollo and G.L. Garagnani, Impact behaviour of A356 alloy for low-pressure die casting automotive wheels, *Journal of Materials Processing Technology*, 209(2), 2009, 1060-1073

[10] 10. L.-t. Jiang, G.-q. Chen, X.-d. He, M. Zhao, Z.-y. Xiu, R.-j. Fan and G.-h. Wu, Microstructure and tensile properties of TiB2p/6061Al composites, *Transactions of Nonferrous Metals Society of China*, 19, Supplement 3(0), 2009, s542-s546

[11] 11. G.K. Sigworth and T.A. Kuhn, Grain Refinement of Aluminum Casting Alloys, *AFS Transactions*, 115(2), 2007, 1-12

[12] 12. C. Wang, M. Wang, Z. Liu, Z. Liu, Y. Weng, T. Song and S. Yang, The grain refining action of fine TiB2 particles in the electrolytic low-titanium aluminum with Al-4B addition, *Materials Science and Engineering: A*, 427(1-2), 2006, 148-153